Effects of Alkylamine Chain Length on the Thermal Behavior of CdSe Quantum Dot Glassy Films

Robert W. Meulenberg, Stephanie Bryan, C. Steven Yun, and Geoffrey F. Strouse*

Department of Chemistry, University of California, Santa Barbara, California 93106

Received: March 20, 2002; In Final Form: June 17, 2002

The competition between dimensional and domain effects for the packing of amphiphilic passivants on CdSe quantum dot (QD) surfaces is examined using temperature-dependent attenuated total reflection infrared spectroscopy. The results indicate that at very small particle sizes ($r < 22$ Å) disordered packing of the organic passivant arises due to the lack of an available thermodynamically stable packing domain for the passivant on the QD facets. At particle sizes $r > 22$ Å, a stable chain domain can be established where the chain packing thermodynamics is governed by purely dimensional effects related to the ratio of the chain length ($\langle L \rangle$) to the particle radius (r). Using a mean field statistical mechanical calculation, we find the theoretical calculations predict the observed $\langle L \rangle / r$ passivant layer stabilization for QD systems.

1. Introduction

The extent to which the stability of a semiconductor quantum dot (QD) is influenced by the area available on a QD facet for surface passivation (domain) and the nature of chain−chain (ch−ch) interactions between the passivants (dimensionality) is an important, but not well understood concept.[1−5] The organic passivant, which typically consists of an organo-phosphine, -thiol, or -amine, is believed to energetically relax defect states via coordination to partially coordinated surface atoms (dangling bonds).[6] The extent of coverage of the surface by the passivant layer, which is nanomaterial type and size dependent, increases the stability of the QD, and is believed to raise the energy of the surface trap states above the band gap, E_g.[7−9] A complete understanding of how the passivant is molecularly oriented on the surface and contributes to the thermodynamic stability of the QD can be useful in understanding the properties of these unique systems.

While the binding of organic passivants on planar self-assembled monolyaer (SAM) surfaces has been well established, the energetics of a molecule adsorbing to a dimensionally restricted or curved surface is more complicated than a large single crystal. Most notably the energetics for dimensional packing of ch−ch interactions are influenced by the ability of the alkyl chains to form a stable crystalline domain on the dimensionally restricted surface. Dimensional effects occur when chain packing on a particle surface experiences an effective increase in its area per headgroup due to changes in packing density at the particle surface, i.e., splaying of the chains at the facet edge, in effect, decreasing packing densities. In nanoscale materials, observations of dimensional effects have been observed in nanocrystals passivated with alkylthiols and amines which show a strong size dependence on the melting enthalpies.[5,10] Domain effects, on the other hand, occur when the surface of a particle is too small to accommodate the kinetically favored domain size of the adsorbing molecules. The appearance of minimum domain structures of organic amphiphiles on bulk SAMs has been well documented.[11] This suggests that as the particle size decreases below a 50 Å facet, the thermodynamic energetics of chain packing may be disturbed and domain effects may be observed for passivant packing in QDs.

In this study, we analyze dimensional and domain effects in CdSe QDs capped with varying alkylamine chain lengths. Using temperature-dependent vibrational spectroscopy coupled to a mean field statistical mechanical calculation, we find that passivant packing on a CdSe QD can be described in terms of both dimensional and domain models. For very small particle sizes ($r < 22$ Å), the available domain size for chain packing is too small for thermodynamic stabilization, resulting in energetically unfavorable packing. At particle sizes above 45 Å, the chain packing thermodynamics is highly dependent on the ratio of the chain length ($\langle L \rangle$) to the particle radius, r. We find a thermodynamic minimum for chain packing at $\langle L \rangle / r \sim 1.0$ when $r > 44$ Å.

2. Experimental Section

2.1. Materials. CdSe QDs were synthesized by a modification of standard lyothermal methods using *n*-hexadecylamine (HDA) as the growth solvent.[12] Crystallinity and size dispersity (∼5−6%) of the materials are monitored by UV−vis absorption pXRD spectroscopies and TEM analysis. $C_{20}H_{43}N$ ligand was synthesized from the corresponding bromide via the Gabriel synthesis. Briefly, the C_{20} alkylamine is synthesized via a nucleophillic attack of potassium phthalimide on the corresponding alkylbromide to obtain the *N*-alkyl phthalimide then subsequently deprotected with hydrazine to afford the desired product.

2.2. Attenuated Total Reflection (ATR) FTIR Spectroscopy. QD samples were dispersed in hexane, deposited on a 4 × 80 mm ZnSe 45° HATR plate (Pike Technologies), and allowed to slowly evaporate. Temperature-dependent ATR-FTIR data were collected on a Perkin-Elmer Spectrum GX system from 650 to 4000 cm^{-1} with a resolution of 2 cm^{-1}. Temperature control between 25 and 100 °C (± 1 °C) was achieved using a manual temperature control (Pike Technologies) coupled to the HATR plate.

3. Theory

The nature of packing for organic amphiphilic molecules on a surface is dependent on the interplay of the ch−ch and the

* To whom correspondence should be addressed. E-mail: Strouse@chem.ucsb.edu.

10.1021/jp025802q CCC: $22.00
Published on Web 07/20/2002

headgroup−surface interactions. Calculations of the free energy of the amphiphilic passivant layer on the surfaces of QDs provides insight into molecular structure, as well as potentially the chemical stability of the passivating layer on the QD surface. The thermodynamic energy for QD passivation by a long chain organic molecule can be described theoretically by adapting a micellar model based on a mean field statistical mechanical approach first developed by Szleifer, Ben-Shaul, and Gelbart.[13−15] The configurational free energy per chain on a QD surface can be described as

$$f_c = \sum_{\alpha} P(\alpha)\epsilon(\alpha) + kT\sum_{\alpha} P(\alpha)\ln P(\alpha) \qquad (1)$$

where $P(\alpha)$ is the probability distribution of chain conformations and $\epsilon(\alpha) = n_g(\alpha)e_g$, where $n_g(\alpha)$ is the number of gauche bonds in chain configuration α, and e_g is the energy of a gauche conformer ($\sim$500 cal mol^{-1}).

The nanoparticle shape is best approximated by assuming a faceted particle shaped as a hexagon, however, when performing the free energy calculations, we "roll-out" the facet to form a sphere with a radius, r. This allows us to calculate the *average* free energy per chain without accounting for difference arising form edge or vertex sites, which will have a higher free energy contribution than the table chains. This assumption produces an average value for the free energy which for larger dots (>40 Å) provides an adequate representation of the surface. The calculation was performed by assuming closest packing of the chains and fixing the chain footprint (fixed by the area-per-headgroup, $\sim$ 20 Å^2) causing the number of chains to scale as r^2. In general, the approximate unit cell lattice parameter of a crystal of alkane chains is $\sim$5.0 Å, [16] which is close to the Cd−Cd spacing in the wurtzite lattice ($\sim$4.3 Å). [17] The differences in site occupation influences the chain tilt which is accounted for by allowing the chains to expand or compress to minimize their free energy. The similarity of the chain and lattice unit cells allows the assumption that the alkyl chains are arranged in a near (1 × 1)-overlayer adsorption configuration on the CdSe(0001) surface. Using the model of Luedtke and Landman,[18] the differences between edge and table lattice sites are modeled of as the difference between boundary and core chains. Luedtke and Landman found that the thermodynamics of boundary and core chains are quite different and dependent on nanocrystal size; however, by averaging over all chains in the nanocrystal and summing over *all* possible chain configurations, we are able to neglect the difference between the two sites.

Assuming the headgroup−surface binding energy remains constant with chain type and dot size, the effects of headgroup−surface free energy contributions to the total free energy is minimal. Adding the size dependent headgroup free energy to the total free energy, as seen in Figure 1 of the Supporting Information, results in drastic deviations in the size dependent free energy and is in contradiction with the experimental observations. This allows $P(\alpha)$ to be calculated by minimizing the free energy subject to the following constraints

$$\sum P(\alpha) = 1 \qquad (2a)$$

$$\langle\phi(x)\rangle = \sum_{\alpha} P(\alpha)\phi(\alpha,x) = a(x) \qquad (2b)$$

where

$$a(x) = \frac{a}{r^2}(x + r)^2 \qquad (3)$$

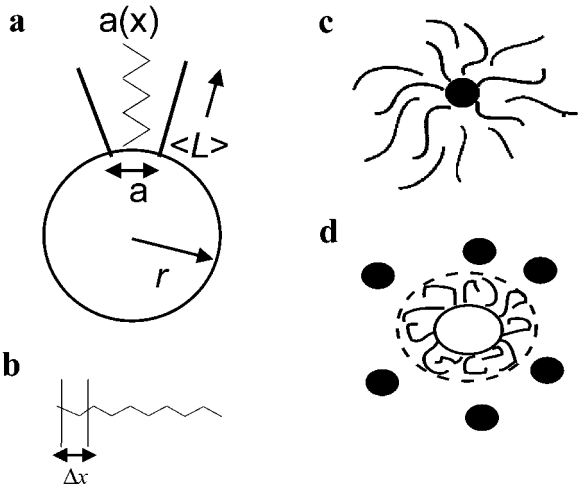

Figure 1. (a) Illustration of the effect of surface curvature or chain splaying on a QD facet where a is the area-per-headgroup, a(x) is the effective area-per-headgroup, $\langle L\rangle$ is the chain length, and r is the particle radius. (b) Illustration of the discrete segments, Δx, to define the long axis of the chain. (c and d) Illustration of the effects of a (c) good and (d) bad solvent.

where $\phi(x)$ is the average density or number of $-CH_2$ groups at a distance x from the surface of the nanoparticle and $a(x)$is the effective area per headgroup due to surface curvature (Figure 1a). This yields an expression for $P(\alpha)$ containing the partition function, z.

$$P(\alpha) = \frac{1}{z}e^{-[\epsilon(\alpha)/kT]-[1/kT]\int \pi(x)\phi(\alpha,x)dx} \qquad (4)$$

where

$$z = \sum_{\alpha} e^{-[\epsilon(\alpha)/kT]-[1/kT]\int \pi(x)\phi(\alpha,x)dx} \qquad (5)$$

To carry out these computations along the x-axis, the axis extending along the radius has been divided into discrete segments, Δx, allowing the above integral to be transformed into a sum of discrete steps, which are effectively related to the number of $-CH_2$ segments (Figure 1b). The terms $\pi(x)$ represent Lagrange multipliers associated with the packing constraints and represent the one-dimensional pressure applied to the chain. The free energy of the ligand layer can be calculated under various conditions (good vs bad solvents) using the Flory parameter, χ,

$$\chi = \frac{1}{kT}[w_{cs} - (w_{cc} + w_{ss})/2] \qquad (6)$$

with w_{cs}, w_{cc}, *and* w_{ss} equal to the chain−solvent, chain−chain, and solvent−solvent interaction potentials, respectively (Figure 1c,d). Systems where chain−chain and chain−solvent interactions are identical are said to be in a "good" or "athermal" solvent with $\chi \ll 1$, and systems where $\chi \gg 1$ are labeled "bad" solvents.[19]

Figure 2 shows the free energy calculation of a C_{12} chain on a QD surface in "good" and "bad" solvents. Based on the mean field calculations, in a "good" solvent, such as hexane, the free energy decreases with decreasing radius (Figure 2a). This result states that for a QD in a "good" solvent condition, the ligand layer is never in a thermodynamically stable conformation. This implies that chain packing will adopt an increasingly crystalline structure with increasing chain length as observed in SAMs, indicative of a passivating layer model that exhibits a *frozen*

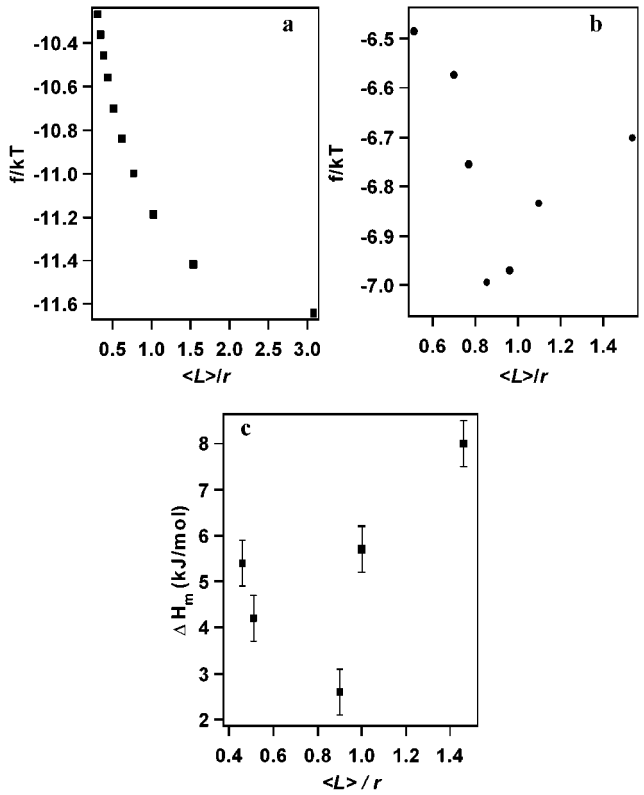

Figure 2. (a, b, and c). Free energy calculation of a C_{12} chain on a QD surface in (a) good and (b) bad solvents and (c) experimental latent heats of melting, ΔH_m, as a function of $\langle L\rangle/r$.

kinetic structure strongly dictated by the headgroup−surface interaction and not dimensional effects. In our earlier thermal and IR analysis of QD films, this behavior was not experimentally observed, suggesting thin film structures are in a "bad" solvent condition.[5]

In a "bad" solvent condition, a minimum in the conformational free energy of the ligand is observed at a "favored size" of $\langle L\rangle/r \sim 0.9$ (Figure 2b). The passivant layer can be envisioned as existing in a thermodynamically favored configuration dominated by ch−ch packing interactions. This means that the passivant layer will experience dimensional effects as the ratio of chain length and particle size varies. These predictions correspond with our earlier findings for chain packing on CdSe QD thin films, allowing our glassy QD film structures self-assembled by solution evaporation to be envisioned as a "bad" solvent condition.[5] Even more interesting, the calculated "favored" size observed in Figure 2b is in quantitative agreement with the observed maximum in enthalpies of melting of dodecanthiolate coated Au nanocrystals reported in ref 10. The theoretically predicted "favored" size $\langle L\rangle/r$ can be thought of as a balance between forces of energy and entropy. At large particle sizes, energy dominates, but at small particle sizes entropy dominates.

A measure of the predicted chain conformation on a QD surface can be achieved by plotting $\phi(x)$ for a given chain length as a function of various QD sizes. Figure 3 shows the calculated values of $\phi(x)$ vs the distance from the QD surface for a C_{12} alkyl chain passivating CdSe. Since $\phi(x)$ represents the average number of $-CH_2$ groups at a distance x from the surface of the QD in a "bad" solvent condition, a value of $\phi(x) = 1.0$ states that an all-trans conformation is achieved by the chain, while a value of $\phi(x) > 1.0$ shows increasing gauche conformational defects on the chain. This produces effective chain compression, and a lower $\langle L\rangle$ value. Coupled to the compression, inclusion

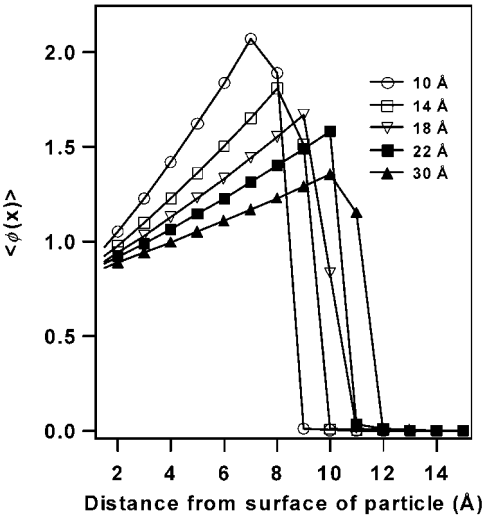

Figure 3. Calculated values of the average density, $\phi(x)$, as a function of distance from the surface of the quantum dot for various QD sizes.

of gauche conformer defects tends to lower packing densities of the passivant layer on the QD surface. Inspection of Figure 3 indicates that a predominately crystalline all-trans conformation for the C_{12} alkyl chain passivating layer is predicted for QD sizes in excess of 20 Å. At particles sizes below 14 Å, the $-CH_2$ density is high, extending only 8 Å from the particle surface when a C_{12} all-trans conformer can extend nearly 15 Å. This means that nearly half of the chain is "curled up" or contains a large amount of gauche defects. From Figure 3, we see that between 18 and 22 Å, the average chain density decreases (i.e. less defects) and the distance from the particle surface increases, reaching a value of nearly 12 Å, showing that the chains are nearing an all-trans, highly crystalline conformation. This gives rise to dimensionality effects arising at the CdSe-passivant $\langle L\rangle/r > 1.0$, for a C_{12} ligand.

Using eq 3, the increase of the area per headgroup, $a(x)$, scales as r^{-2} implying that an increase of $a(x)$ occurs at small particle sizes and most likely leads to the increase in gauche conformers. This leads to an expected increase in chain splaying on the surface to maximize area at the expense of chain packing. As the particle radius increases, the "effective" area per headgroup, $a(x)$, tends toward the "normal" area per headgroup, a, inducing restricted movements of the surface bound ligands. The restricted movements results in strong ch−ch van der Waals interactions and all-trans packing motifs as predicted from the large $\phi(x)$ values (Figure 3) and the increase in $\pi(x)$ (Figure 2 of the Supporting Information).

Experimental verification of the dimensional predictions can be generated by comparison of the theoretical calculations for the passivant layer and the experimental melting passivant layer behavior on a QD surface measured by differential scanning calorimetry (DSC). From the DSC measurements, the energy required to melt the chains via gauche conformer formation can be directly measured. This provides a comparable value of the configurational free energy for chain melting at given $\langle L\rangle/r$ values. Using the calculated free energy seen in Figure 2b and the experimental latent heats of melting, ΔH_m, measured by DSC, a correlation is observed between $0.9 < \langle L\rangle/r < 1.0$ in the free energy and latent heats of melting (Figure 2c). The experimental validation of the theoretical predictions suggest after the free energy minimum is reached packing constraints lead to an increase in configurational free energy for the passivant layer. In Figure 3, where the value for $\phi(x)$ decreases as $\langle L\rangle/r > 1.0$, an increase of gauche conformers of the chain

on the surface of the QD is predicted, arising from changes in packing density on the QD surface. As the energy for a gauche conformer is only ~22 meV, it is expected that for systems where there is sufficient volume and/or greater rotational degrees of freedom, an increase in gauche conformers would be expected.

4. Dimensional vs Domain Effects

In a previous study on chain packing and chain dynamics on a QD surfaces, the influence of QD size was investigated by a correlation of the thermal melting behavior and temperature-dependent IR properties for a series of QDs.[5] In this study, it was observed that changes in chain tilting and conformational integrity were experienced for QDs below a radius of 25 Å. These changes were ascribed to dimensionality effects on QD surfaces arising from changes in the enthalpic ch−ch stabilization, as well as enhanced headgroup−surface interactions. These results are analogous to the observation of reduced dimensionality effects on Au nanoparticles.[10,20,21]

The statistical mechanical model above predicts a $\langle L \rangle / r$ dependence. This dimensional model predicts the stability of alkyl chains on the surface of size restricted particles will be directly related to the ratio of chain length to QD size needed to minimize the conformational free energy of the chains. If a particle is very small, the surface area becomes much smaller resulting in increased chain splaying and therefore fewer chains effectively pack on the surface. This will tend to decrease the thermodynamic stability of the particle. In light of the earlier studies, this predicts analysis of the DSC and temperature-dependent IR will provide direct insight in to the validity of the theoretical model.

By analysis of conformationally sensitive IR modes, the theoretical model can be experimentally verified. A measure of the crystallinity for an alkyl chain can be attained by inspection of the frequency and line width of the spectral region between 2800 and 3100 cm^{-1}. This region can be assigned to contributions from the ν_{CH} stretching modes (d^+, d^-) for $-CH_2$ along the polymethylene alkylamine chains and to the end-methyl groups ($-CH_3$) (r^+, r^-). These modes are highly dependent on the chain crystallinity and packing conformation of the alkylamine chains assembled on the QD surface.[5,22−24] Observation of the d^+ and d^- modes between 2848 and 2850 and 2914−2916 cm^{-1} are consistent with an assignment of a predominately all-trans packing arrangement at the surface of a QD, with a shift of these mode frequencies occurring with the onset of gauche conformers. The band observed at ~3331 cm^{-1} arises from the N−H asymmetric stretch which loses intensity with increasing size and can be attributed to changes in chain tilt on the surface of the QD. As the chain tilts, the intensity of the NH mode increases, due to loss of surface selection rules. Coupled to the loss of the NH modes, splitting of the r^+/r^- modes can be observed due to symmetry breaking. Coupled to these IR signatures, "twist and wag" (T_x and W_x) progressions between 1150 and 1350 cm^{-1} can be observed indicative of high packing densities for all trans-conformations. Furthermore signature modes for hexagonal packing on the QD surface are observed at 720 (P_1) and 1470 (δ) cm^{-1} in CdSe passivated with alkylamines.

The purely dimensional model is clearly observed for $\langle L \rangle / r < 1.0$. for example. a 70 Å CdSe particle passivated with HDA, where the chain packing motif is hexagonal and highly crystalline with clearly resolved "twist and wag" (T_x and W_x) progressions (Figure 4). For the 70 Å CdSe QD, loss of intensity for the NH mode and a splitting of the methyl modes is

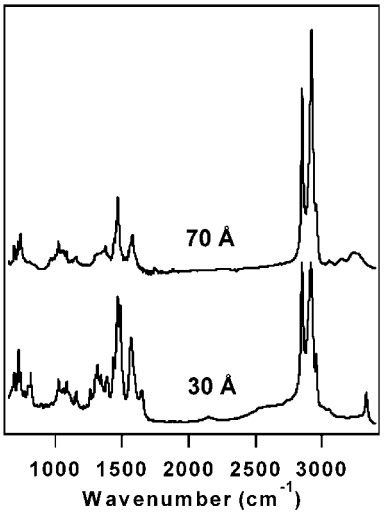

Figure 4. Room temperature infrared absorption between 700−3100 cm^{-1} of 70 and 30 Å CdSe QDs coated with HDA.

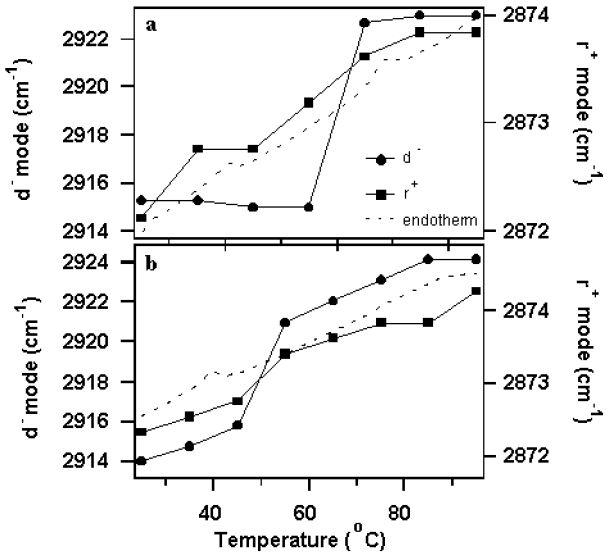

Figure 5. (a and b). Thermal behavior of the methylene (d^-) and methyl (r^+) modes and corresponding DSC traces for the (a) 70 and (b) 30 Å CdSe QD glassy films passivated with hexadecylamine. Note the correlation between the shifts of the d^- and r^+ peaks with the endothermic transitions.

indicative of chain tilting in these materials. This suggests in this size regime, the chain length compensates for the particle surface effects and the thermodynamics are entirely dominated by ch−ch enthalpic terms. For $\langle L \rangle / r > 1.0$, for example, a 30 Å CdSe particle passivated with HDA, the reduced dimensionality of the CdSe QD allows for greater rotational degrees of freedom of the surface groups, and onset of chain tilting as evidenced by the observation of the NH mode at 3331 cm^{-1}, and a loss of the methyl mode splitting. The change in tilting and chain freedom arises from an effective lower packing density for the passivants.

The thermal analysis data, obtained by DSC measurements, confirm these observations with a two-step melting behavior for 70 Å CdSe and a one-step curve for the 30 Å CdSe. In Figure 5, a comparison of the thermal behavior of the methylene (d^-) and methyl (r^+) modes is shown for the 30 and 70 Å QD films passivated with hexadecylamine (HDA; $\langle L \rangle \sim 21$ Å). The two-step melting behavior arises from strong ch−ch interactions in the packing resulting in an initial end-gauche formation with heating, followed by complete chain collapse at elevated

temperature. For the 70 Å CdSe materials, the onset of melting is observed initially for the methyl IR mode ($\nu_{CH_3} \sim 2850$ cm^{-1}), which is shifted to higher frequency upon heating, and a delayed frequency shift for the methylene IR mode ($\nu_{CH_2} \sim 2916$ cm^{-1}), implying the onset of end-gauche and internal gauche conformers are not thermodynamically equivalent (Figure 5a). Coupled to the onset of the intrachain gauche defects is increased conformational disorder as evidenced by the loss of intensity from the T_x and W_x progression series modes as a function of temperature.[25] In contrast, the 30 Å CdSe QD with a C_{16} passivating layer exhibits a correlated melting event with loss of crystallinity occurring simultaneously with end-gauche formation, explaining the one-step melt event. Above the melting phase transition temperature (>50 °C), a quasi-linear hardening of the modes is observed consistent with collapse of the alkyl chains. As the 30 Å assembly is heated, ν_{NH_2} begins to lose intensity at ~328 K (55 °C) indicating that the mechanism for chain collapse on small particles involves chain canting followed by chain collapse.

The magnitude of the frequency shift in the antisymmetric $-CH_2$ stretch (d^- mode) is 10.0 and 4.0 cm^{-1} for the 30 and 70 Å QD assemblies, respectively (Figure 5). The smaller $\Delta\nu$ value for the 70 Å assemblies leads to the assumption that packing is more constrained on these particles as seen in the two-phase melt behavior, with end methyl free rotation (~315 K) occurring in a thermodynamically separate event than the methylene chain collapse event (~345 K). Evidence for a tightly packed state is also seen in the lack of $-NH_2$ absorption at ~3330 cm^{-1} implying an all-trans, densely packed motif. The differences in the magnitude of the shifts implies the 30 Å assembly is able to achieve a more liquid like disordered collapse state, in comparison to the 70 Å dot, most likely due to the increased effective curvature for the size restricted surface. These results can be interpreted in terms of dimensionality effects ($1 > \langle L\rangle/r > 1$) as predicted theoretically.

4.1. Experimental Validity of Dimensionality. A test for the validity of the dimensionality model can be determined by inspection of the thermal behavior for various chain lengths for a given QD size. The onset of dimensional effects is observable by inspection of the temperature-dependent IR and analysis of the methyl and methylene modes. A system exhibiting dimensional stress will exhibit a one-step melting curve ($\langle L\rangle/r > 1$), while systems without dimensional stress ($\langle L\rangle/r < 1$) are expected to exhibit a two-step melting event in which the chain packing will be dominated entirely by the ch−ch interactions. Chain lengths of 27 carbon atoms would be needed to induce dimensional effects to a 70 Å ($r = 35$ Å) particle. For a 30 Å ($r = 15$ Å) particle, however, chain lengths of 11 carbon atoms or more would be needed to induce dimensional effects ($\langle L\rangle/r < 1$). This suggests for chain lengths shorter than C_{12}, dimensional effects will be absent in both of the systems, while for C_{16} passivation dimensional effects for the 30 Å dots are most crucial, predicting a change in the packing and thermotropic properties should be observable.

The influence of dimensionality on packing for a series of chain lengths on a 70 Å particle exhibits a two-step melting curve similar to C_{16} coated QDs for all chain lengths >C_8 (C_8, C_{12}, C_{16}, and C_{20}). These chain lengths are within the $\langle L\rangle/r < 1$ regime for chain packing, which means the packing of the chains will be dominated by strong ch−ch interactions and at room temperature the crystallinity will be largely influenced by the number of available ch−ch interactions (Figure 6). Consistent with ch−ch interactions dominating the packing for systems in the $\langle L\rangle/r < 1$, for chain lengths <C_5 on a 70 Å QD

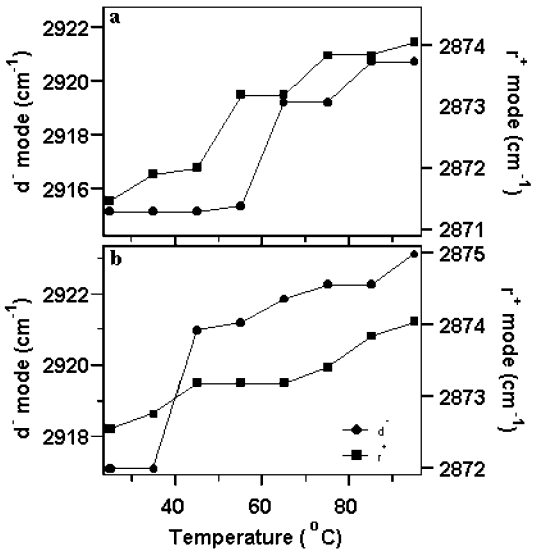

Figure 6. (a and b). Thermal behavior of the methylene (d^-) and methyl (r^+) modes for 70 Å CdSe QD glassy films passivated with (a) eicosamine and (b) dodecylamine.

disordered packing is observed. The C_5 chain can be envisioned as in a melt state at room temperature on the surface, with a loss of structural regularity arising from the minimal available contribution of ch−ch interactions to stabilize the passivant layer on the surface. For the C_5 system, the lack of crystalline order is clearly seen in the frequency of the CH_2 modes, which is shifted to higher frequency indicative of an increase in gauche conformer concentrations along the chain. Consistent with the increased gauche conformations, the lack of shifts in the $d^{+/-}$ modes with temperature and the lack of peaks at 720 (P_1) and 1470 (δ) cm^{-1} which are signature packing modes, suggest the chains are randomly oriented on the QD surface. These studies indicate that at large quantum dot sizes (large r), dimensionality effects may be minimal due to $\langle L\rangle/r$ typically being less than 1. In effect, adsorbed molecules experience a quasi-planar surface with respect to the chain length and mimic the observation of organic passiavting layers in self-assembled monolayers.

Dimensionality effects on the other hand for small QD sizes should be observed as $\langle L\rangle/r$ can be systematically tuned. Using the above dimensional model, a one-step melt transition at $\langle L\rangle/r \geq 1.0$ is predicted for a $C_n > C_{12}$ ($\langle L\rangle \sim 15.4$ Å) chain length on a 30 Å QD and a two-step melting curve for chain lengths below C_{12}. Surprisingly, the observation of a one-step melt for 30 Å QDs passivated with HDA ($\langle L\rangle \sim 20$ Å), dodecylamine (DDA, $\langle L\rangle \sim 15$ Å), or octylamine (OA, $\langle L\rangle \sim 10$ Å) indicates purely dimensional effects do not accurately describe the packing of the passivant molecules on a surface for these smaller QDs (Figure 7). Based on the 30 Å CdSe−DDA d^- mode frequency of 2917 cm^{-1} compared to the value of 2914 cm^{-1} for 30 Å CdSe−HDA and 2917 cm^{-1} for CdSe−OA, an insignificant loss of crystallinity in the packing arises as the chain length decreases, in contrast to the expected behavior for a purely dimensional model (Figure 8). Furthermore, the HDA, DDA, and OA coated dots show $\nu_{NH_2} \sim 3330$ cm^{-1} with their peak positions differing by less than 1%. These materials all exhibit similar thermal behavior suggesting that packing on a 30 Å QD varies little with chain length in contrast to prediction of a purely dimensional model. The lack of a two-step melt event for the DDA and OA coated dots puts a purely dimensional model in jeopardy. This suggests that the small particle size may affect the chain packing by limiting the ability to form a stable crystalline domain on the QD facet. The

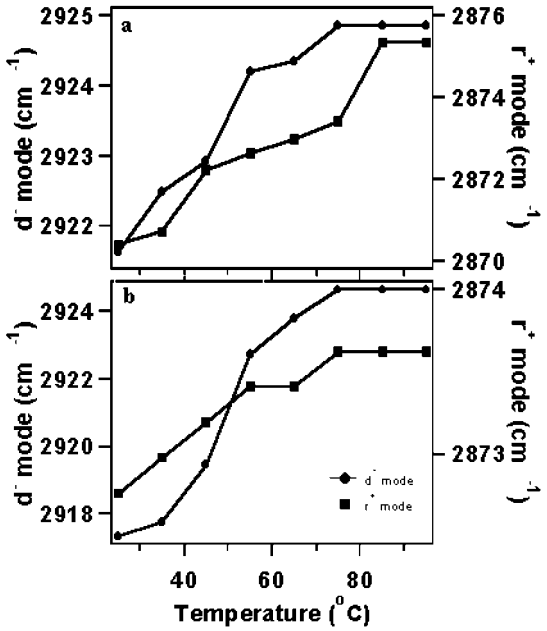

Figure 7. (a and b). Thermal behavior of the methylene (d^-) and methyl (r^+) modes for 30 Å CdSe QD glassy films passivated with (a) octylamine and (b) dodecylamine.

evidence of no apparent two-step melt on small dots makes it necessary to describe the phase behavior of the alkyl chains in a different way, perhaps in terms of domain structures.

4.2. Domain Effects on QD Passivation. Domain induced packing stress in materials without a large facet may arise due to the limited number of Cd lattice points on a facet for a passivating layer to interact with. At a low packing density, the ch−ch interactions are not strong enough to overcome the limited crystalline domain available. In SAMs, the observed minimum domain size of organic passivants is on the order of 40−50 Å. In Au SAMs, chain domain sizes of 40−50 Å are equivalent to 14−17 Au unit cells.[26] The same observations on nanoscale surfaces have not been clearly identified, but have been indirectly observed. Korgel and Fitzmaurice have observed that chain stabilization on Ag nanocrystals is highly sensitive to the $\langle L\rangle/r$ ratio, and the free energy minimum occurs at $\langle L\rangle/r \sim 0.60$.[27] The obtained ratios are the same for C_{12} and C_8 coated nanocrystals and their ratios are similar to the values obtained by Whetten and co-workers.[28] Thermodynamic stabilization in light of domain size was never discussed, mainly from the fact that the smallest sized nanocrystal used in these studies were ∼36 Å, which represent ∼10 Ag unit cells ($d_{Ag-Ag} \sim 2.88$ Å),[29] more than enough unit cells for chain stabilization.

TABLE 1: Minimum Observed Domain and the Correlating Number of Repeat Unit Cells of Alkanethiols on Au(111) Surfaces[a]

chain length	average domain size (Å)	no. of alkyl unit cells
C_{18}	35.2	7
C_{14}	43.9	9
C_{10}	36.4	7

[a] Reference 25.

TABLE 2: Effective Facet Dimension and Number of Repeat Unit Cells on the Wurtzite CdSe (0001) Face

particle radius (Å)	facet dimension (Å)	no. of Cd−Cd unit cells
16	27.7	6.4
22	38.7	9.0
35	60.6	14.1

An interesting observation by Lennox and co-workers was made on alkanethiolate coated Au nanocrystals.[30,31] They found that the local Au−S bonding was the same on the nanocrystal as seen on bulk Au SAMs. This only occurred, however, for particle sizes larger than 22 Å where the number of Au unit cells is ∼7 ($d_{Au-Au} \sim 2.88$ Å),[29] just at the threshold for the minimum alkyl chain unit cells needed for stabilization. These results indicate that below 22 Å, Au nanocrystals may lack the effective domain size needed to reach a kinetically favorable chain unit cell dimension. This provides indirect evidence for the existence of domain effects in nanomaterial packing.

The influence of domain limitations for CdSe particles <30 Å can be interpreted in terms of the number of required repeat unit cells to form a stable crystalline domain on a surface. The alkyl chain domain size is kinetically driven and has an average size of ∼40 Å, which corresponds to approximately 8 repeat alkyl chain unit cells (Table 1).[16] In comparison, Table 2 shows the repeat Cd−Cd unit cells which vary from 6 (32 Å) to 14 (70 Å). These numbers can be compared against known domain sizes of alkanethiols on Au(111) surfaces[26] to compare the number of unit cells available in the CdSe(001) lattice for packing versus the kinetically favored number of alkanethiol unit cells required for stabilization (Tables 1 and 2). It is seen

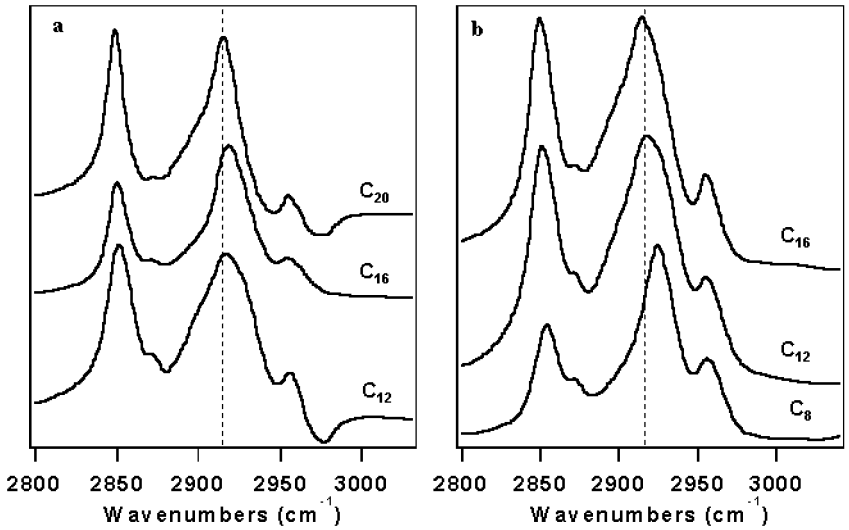

Figure 8. (a and b). Room temperature infrared absorption between 2800−3100 cm^{-1} of (a) 70 Å CdSe QDs coated with H_2NC_{20}, H_2NC_{16}, and H_2NC_{12} and (b) 30 Å CdSe QDs coated with H_2NC_{16}, H_2NC_{12},

that approximately 7−9 alkyl unit cells are needed for stabilization. In contrast, only ~6 unit cells are available for packing in a 32 Å dot versus ~14 unit cells in a 70 Å dot. Not surprisingly, a 44 Å particle is needed to achieve 9 CdSe unit cells which is minimum size needed for thermodynamic stabilization of the chains and it occurs precisely where we witnessed a change in the melting behavior of HDA coated dots in ref 5. These results along with the previous experiments on Au nanocrystals provide evidence for the existence of domain sizes in QDs, suggesting QD instability arising from loss of the passivating layer may arise for QDs having fewer available passivant binding sites per facet. This suggests that for CdSe, particle sizes of 45 Å or greater should be used for materials' applications, as these appear to be the most energetically stable sizes.

5. Conclusions

In conclusion, we find that amphiphilic passivant packing on a CdSe QD can be described in terms of both dimensional and domain models. The results indicate that at very small particle sizes ($r < 22$ Å) disordered packing of the organic passivant arises due to the lack of an available domain size for chain packing on the faceted QD surface. This results in increased chain splaying to maximize chain crystallinity and particle stabilization. At particle sizes above 45 Å, the chain packing thermodynamics is highly dependent on the ratio of the chain length ($\langle L \rangle$) to the particle radius, r, with a thermodynamic minimum for chain packing at $\langle L \rangle / r \sim 1.0$. These results indicate that ligand exchange kinetics on these particles should be highly size dependent and sensitive to dimensional and domain effects. Such studies are currently underway.

Acknowledgment. This work was supported by a NSF-CAREER Award (DMR-9875940) and a NSF Nanotechnology Grant (DMR-9871849).

Supporting Information Available: Figure 1: Calculated values of f_c with the phenomenological headgroup free energy f_h. Figure 2: Calculated values of $\pi(x)$ with the negative values of $\pi(x)$. This material is available free of charge via the Internet at http://pubs.acs.org.

References and Notes

(1) Katari, J. E. B.; Colvin, V. L.; Alivisatos, A. P. *J. Phys. Chem.* **1994**, *98*, 4109−4117.

(2) Prozorov, T.; Gedanken, A. *Adv. Mater.* **1998**, *10*, 532−535.

(3) Cordero, S. R.; Carson, P. J.; Estabrook, R. A.; Strouse, G. F.; Buratto, S. K. *J. Phys. Chem. B* **2000**, *104*, 12137−12142.

(4) Kim, B. S.; Avila, L.; Brus, L. E.; Herman, I. P. *Appl. Phys. Lett.* **2000**, *76*, 3715−3717.

(5) Meulenberg, R. W.; Strouse, G. F. *J. Phys. Chem. B* **2001**, *105*, 7438−7445.

(6) Murray, C. B.; Norris, D. J.; Bawendi, M. G. *J. Am. Chem. Soc.* **1993**, *115*, 8706−8715.

(7) Alivisatos, A. P. *J. Phys. Chem.* **1996**, *100*, 13226−13239.

(8) Bawendi, M. G.; Carroll, P. J.; Wilson, W. L.; Brus, L. E. *J. Chem. Phys.* **1992**, *96*, 946−954.

(9) Becerra, L. R.; Murray, C. B.; Griffin, R. G.; Bawendi, M. G. *J. Chem. Phys.* **1994**, *100*, 3297−3300.

(10) Hostetler, M. J.; Wingate, J. E.; Zhong, C. J.; Harris, J. E.; Vachet, R. W.; Clark, M. R.; Londono, J. D.; Green, S. J.; Stokes, J. J.; Wignall, G. D.; Glish, G. L.; Porter, M. D.; Evans, N. D.; Murray, R. W. *Langmuir* **1998**, *14*, 17−30.

(11) Dubois, L. H.; Nuzzo, R. G. *Annu. Rev. Phys. Chem.* **1992**, *43*, 437−463.

(12) Cumberland, S. L.; Hanif, K. M.; Javier, A.; Khitrov, G. A.; Strouse, G. F.; Woessner, S. M.; Yun, C. S. *Chemistry of Materials* **2002**, *14*, 1576−1584.

(13) Gelbart, W.; Ben-Shaul, A.; Roux, D. *Micelles, Membranes, Microemulsions, and Monolayers*; Springer-Verlag: New York, 1994.

(14) Steenhuizen, L.; Kramer, D.; Benshaul, A. *J. Phys. Chem.* **1991**, *95*, 7477−7483.

(15) Heath, J. R.; Knobler, C. M.; Leff, D. V. *J. Phys. Chem. B* **1997**, *101*, 189−197.

(16) McGann, M. R.; Lacks, D. J. *J. Phys. Chem. B* **1999**, *103*, 2796−2802.

(17) D. R. Lide, D. R., Ed. *CRC Handbook of Chemistry and Physics*; CRC Press: Boca Raton, 1993; Vol. 74.

(18) Luedtke, W. D.; Landman, U. *J. Phys. Chem.* **1996**, *100*, 13323−13329.

(19) Szleifer, I.; Ben-Shaul, A.; Gelbart, W. M. *J. Phys. Chem.* **1990**, *94*, 5081−5089.

(20) Badia, A.; Cuccia, L.; Demers, L.; Morin, F.; Lennox, R. B. *J. Am. Chem. Soc.* **1997**, *119*, 2682−2692.

(21) Hostetler, M. J.; Stokes, J. J.; Murray, R. W. *Langmuir* **1996**, *12*, 3604−3612.

(22) Nielsen, J. R.; Hathaway, C. E. *J. Mol. Spectrosc.* **1963**, *10*, 366−377.

(23) MacPhail, R. A.; Strauss, H. L.; Snyder, R. G.; Elliger, C. A. *J. Phys. Chem.* **1982**, *86*, 5145−5150.

(24) Parikh, A. N.; Gillmor, S. D.; Beers, J. D.; Beardmore, K. M.; Cutts, R. W.; Swanson, B. I. *J. Phys.Chem. B* **1999**, *103*, 2850−2861.

(25) Bardeau, J. F.; Parikh, A. N.; Beers, J. D.; Swanson, B. I. *J. Phys. Chem. B* **2000**, *104*, 627−635.

(26) Camillone, N.; Chidsey, C. E. D.; Liu, G. Y.; Putvinski, T. M.; Scoles, G. *J. Chem. Phys.* **1991**, *94*, 8493−8502.

(27) Korgel, B. A.; Fitzmaurice, D. *Phys. Rev. B: Condens. Matter* **1999**, *59*, 14191−14201.

(28) Whetten, R. L.; Shafigullin, M. N.; Khoury, J. T.; Schaaff, T. G.; Vezmar, I.; Alvarez, M. M.; Wilkinson, A. *Acc. Chem. Res.* **1999**, *32*, 397−406.

(29) Laibinis, P. E.; Whitesides, G. M.; Allara, D. L.; Tao, Y. T.; Parikh, A. N.; Nuzzo, R. G. *J. Am. Chem. Soc.* **1991**, *113*, 7152−7167.

(30) Badia, A.; Lennox, R. B.; Reven, L. *Acc. Chem. Res.* **2000**, *33*, 475−481.

(31) Bourg, M. C.; Badia, A.; Lennox, R. B. *J. Phys. Chem. B* **2000**, *104*, 6562−6567.